On Some Aspects of Initialization and Forecasts in the Indian Monsoon Region

S. S. SINGH, A. A. KULKARNI AND D. R. SIKKA

Indian Institute of Tropical Meteorology, Poona-5, India

(Manuscript received 30 July 1979, in final form 30 January 1980)

ABSTRACT

Application of a dynamic initialization scheme for balancing initial wind and pressure fields for a one-level primitive equation model in the Indian region has been investigated. For this purpose, the model equations are integrated forward and backward around the initial time following the Euler backward time-difference scheme without restoration of any variable. For comparison, the initial wind-pressure balance has also been constructed from the observed horizontal motion field by a hierarchy of models of increasing complexity, using the geostrophic relation, the linear balance equation and the nonlinear balance equation. Furthermore, the 48 h forecasts are prepared using the balanced initial data derived from the static nonlinear balance equation and the dynamic initialization scheme. The forecast results from both initialization schemes are compared and discussed. The results obtained from the dynamic initialization scheme are found to be either slightly superior or comparable to those based on the static initialization scheme.

1. Introduction

The solution of the primitive equation system is very sensitive to the state of initial balance between wind and pressure fields. The subjective or objective analyses used for deriving wind and pressure fields often show large imbalances between Coriolis and pressure gradient forces which lead to large-amplitude inertio-gravity waves if the primitive equations are integrated using such initial data. The large-scale atmospheric motions are normally in quasi-nondivergent hydrostatic balance and small-scale fluctuations are rapidly restored toward a balanced state through the adjustment processes and by dissipative forces. Thus, a state of balance between wind and pressure fields is a basic prerequisite of initial data. Geostrophic approximation is the simplest relation between wind and pressure. However, Charney (1955) showed that use of the geostrophic relation for primitive equation initialization may result in noticeable noise and alternatively suggested the use of the nonlinear balance equation to relate the initial wind and pressure fields. Hinkelmann (1959) and Phillips (1960) demonstrated that the use of the geostrophic or balance equation to relate the initial wind and pressure fields for primitive equations integration will result in contamination of meteorological field, especially in a baroclinic atmosphere. However, the balance equation has been widely used for initialization in one-level and multilevel primitive equation models and the noise level in actual integration is suppressed by low-pass filters or high viscous dissipation. Another method of initialization which uses primitive equations directly has been developed by Miyakoda and Moyer (1968) and Nitta and Hovermale (1969). This method is known as dynamic initialization. In this approach, the data for dominant variables are inserted into the prognostic equations and the balanced conditions are achieved by integrating the system of equations back and forth by using numerical analogs which tend to suppress the gravity waves but do not affect the meteorological component significantly. A great deal of research over the past few years has been devoted to the application of dynamic initialization schemes for the primitive equation. Mesinger (1972) and Winninghoff (1973) have advocated the use of a multi-time level forward-backward iteration scheme instead of a single time level scheme. Mesinger concluded that the solution converges rapidly by the multi-time level method. Following Mesinger (1972) and Winninghoff (1973), Kanamitsu (1975) and Kiangi (1977) have used the dynamic initialization scheme of the multi-time level forward-backward iteration in their numerical models for the tropical region.

A third technique of balancing mass and motion fields, known as normal mode initialization, has been developed recently and considerable studies have been reported (Williamson and Dickinson, 1976; Machenhauer, 1977; Baer, 1977; Baer and Tribbia, 1977). The normal mode initialization is based on the idea of expanding initial data into normal modes or free oscillations of linear or nonlinear versions of the model. The model amplitude thought to be unrealistically large can be set to zero

0027-0644/80/091315-11$06.75

or considerably reduced. Studies have shown that the technique is useful for numerical weather prediction with a global model, particularly effective in lower latitudes. However, the technique is not necessarily convenient for regional prediction and for the latter purpose the static and dynamic initialization schemes are still usable.

For the Indian region, the balance equation initialization (static initialization) has been successfully applied for a one-level primitive equation model by Ramanathan and Saha (1972) for predicting the movement of western disturbances and by Singh and Saha (1976) and Singh (1977) for forecasting movement of monsoon depressions and tropical cyclones. The object of the present study is to discuss the applicability of the dynamical initialization scheme and assess whether it can really yield higher quality forecasts than the conventional balance scheme for synoptic-scale disturbances in the summer monsoonal flow. For this purpose, we propose to use primitive equations relevant to the divergent barotropic model for dynamic initialization following Winninghoff (1973) and Kanamitsu (1975). In addition, the initial balance data have also been constructed from the observed motion field by a hierarchy of models of increasing complexity using the geostrophic relation, the linear balance equation and the nonlinear balance equation and compared with the dynamically initialized balance state. Furthermore, the model equations are integrated up to 48 h using the data derived from static and dynamic initialization schemes and the salient features of the differences among the two sets of forecasts are discussed.

2. Methods of computation

a. Model equations

In the case of a divergent barotropic model the prediction equations (shallow water equations) for the three unknown u, v and h in a Cartesian coordinate system on Mercator projection are

$$\frac{\partial u}{\partial t} + m\left(u\frac{\partial u}{\partial x} + v\frac{\partial u}{\partial y} + g\frac{\partial h}{\partial x}\right) - fv = 0, \quad (1)$$

$$\frac{\partial v}{\partial t} + m\left(u\frac{\partial v}{\partial x} + v\frac{\partial v}{\partial y} + g\frac{\partial h}{\partial y}\right) + fu = 0, \quad (2)$$

$$\frac{\partial h}{\partial t} + m\left[u\frac{\partial h}{\partial x} + v\frac{\partial h}{\partial y} + h\left(\frac{\partial u}{\partial x} + \frac{\partial v}{\partial y}\right)\right] - vh\frac{\partial m}{\partial y} = 0, \quad (3)$$

where u, v are the components of the horizontal velocity vector (u along the x coordinate pointing eastward and v along the y coordinate pointing northward), h the height of a free surface ($h = 0$ is the mean sea level), t time, g acceleration due to gravity, m the map factor (secant of latitude) and f the Coriolis parameter. This system of equations allows as solutions external gravity waves which can grow spuriously due to certain imbalance in the mass and velocity field. Thus, initialization schemes are required to suppress the spurious growth of gravity waves.

b. Static initialization schemes

The basic input to the model is the wind field. The streamfunction (ψ) is obtained from the observed wind by solving

$$\nabla^2\psi = m^2\left[\frac{\partial}{\partial x}\left(\frac{v}{m}\right) - \frac{\partial}{\partial y}\left(\frac{u}{m}\right)\right]. \quad (4)$$

The boundary conditions for the solution of the above equation are discussed subsequently.

From the computed ψ field u and v are obtained by using the relations $u = -\partial\psi/\partial y$; $v = \partial\psi/\partial x$. Four types of balance field are obtained from the observed horizontal wind field by static initialization:

SCHEME I: Geostrophic relation with f constant

$$\nabla^2(gh) = \nabla^2(\bar{f}\psi). \quad (5)$$

SCHEME II: Geostrophic relation with f variable

$$\nabla^2(gh) = \nabla^2(f\psi). \quad (6)$$

SCHEME III: Linear balance equation

$$\nabla^2(gh) = \nabla\cdot(f\nabla\psi). \quad (7)$$

SCHEME IV: Nonlinear balance equation

$$\nabla^2(gh) = \nabla\cdot(f\nabla\psi) + 2J\left(\frac{\partial\psi}{\partial x}, \frac{\partial\psi}{\partial y}\right), \quad (8)$$

where ∇ and ∇^2 are the gradient and Laplacian operators, respectively, and J is Jacobean notation.

c. Scheme V: Dynamic initialization scheme

In this method, the model equations are simultaneously integrated for achieving mutual adjustment between the mass and the wind fields. The method adopted follows 10 time steps forward and backward (from now on this will be called one iteration) using Euler backward time-difference scheme with one predictor and one corrector. The scheme is carried out using the initial observed wind (u,v) and height (h) derived from the nonlinear balance equation (Scheme IV). The above operation is repeated nine times, equivalent to 180 time steps of integration. No consideration is given to the restoration of any variable. Since there is no theoretical criteria for convergence of the scheme, the root-mean-square difference of two successive

iterations are computed for u, v and h fields. The purpose of this exercise is to permit the motion of mass field to adjust to an equilibrium which may depart somewhat from the usual balance laws. The final stage of the balance is appropriately checked to ensure the suppression of inertio-gravity waves. The end product thus achieved gives a desirable wind-pressure relationship for the low latitudes.

The parcel's invariant quantities for the closed system (1)–(3) are potential vorticity $[(f + \zeta)/h]$ and all its powers and the total energy $\frac{1}{2}h(u^2 + v^2 + gh)$, where ζ is the relative vorticity. Therefore, the application of this scheme must ensure near invariance of these quantities. This has been done in this study by choosing suitable finite-difference analogs. In addition, the mean absolute value of velocity divergence has also been constructed for the whole domain and for the area covered by the synoptic-scale cyclonic circulation under consideration within the domain to check the quality of initialization.

d. Finite-difference scheme and the boundary conditions

In the numerical solutions of (1)–(8) care has been taken to use the finite-difference scheme suggested by Shuman (1962) throughout.

For a limited area prediction model, the lateral boundary condition always poses a serious problem. One of the ways to tackle this difficulty is to make east-west cyclic continuity and to place a rigid wall at the north-south boundaries. The same has been adopted for this study. The details of the scheme are as follows: For the east-west cyclic continuity eight extra grid points are used in the zonal direction on the eastern side and the variables are specified as

$$Q(L + 8) = Q(2) \quad \text{and} \quad Q(1) = Q(L + 7),$$

where L is the number of grid points in the east-west direction in the unextended domain and Q stands for any variable such as u, v and h. Data in the extended domain are obtained by fitting a cubic polynomial using values of grid points $L - 1$, L, $L + 7$ and $L + 8$. The north-south boundaries are treated as rigid walls by placing constant values of h at the northernmost and southernmost rows for the solutions of (5)–(8). For this purpose a constant value of streamfunction was specified at southern boundary. The north-south gradients of the streamfunction were set to agree with the smooth variation in the basic current and the streamfunction at the northern boundary was thus computed. The corresponding values of height were computed in the quasi-geostrophic sense.

For the purpose of numerical integration of (1)–(3) the north-south boundaries are also treated as rigid walls in a different way. The wall is placed between the two outermost rows. This is done by setting the normal component of the wind (v) at the two outermost rows equal and opposite of the values of v at one grid inside. The height of the free surface is calculated using the geostrophic relation. For the purpose of forecasting the first forward and, subsequently, centered-difference scheme is adopted for marching in time. The computational scheme is the same as followed in the earlier study by Singh and Saha (1976).

As the domain is artificially extended on the eastern side for the purpose of bringing cyclic continuity, the eight eastern grid points are not included for the presentation of final results. Similarly, the outermost rows in the north-south direction are also excluded, while presenting the results since these values are extrapolated from inside.

The domain of integration extends from 6 to 36°N and 56 to 106°E. A 2° latitude-longitude grid is used in both the cases.

e. Preparation of forecast

Integration of (1)–(3) is carried out up to 48 h using the initial-balance data obtained from the solution of nonlinear balance equation and dynamic initialization. For both cases the invariant quantities of the model for the entire domain are computed at every 6 h of integration in order to ensure the quality of numerical integration. The forecasts are prepared up to 48 h.

3. Data

For the present study, two typical synoptic situations dominated by a monsoon depression, (4 and 5 August 1968) have been selected. Since input to the model is wind, the manual analysis of streamlines and isotachs are done for 0000 GMT at 700 mb in both cases. Singh and Saha (1976) have given justification for selecting the 700 mb level for the summer monsoon flow forecast. Fig. 1 presents the 700 mb wind vector field at 0000 GMT 4 August 1968. A time step of 5 min is found suitable for this purpose for the choice of grid distance. The mean height of the free surface is taken as 2000 gpm corresponding to 700 mb. This value is little higher than the one used by Singh and Saha. However, 2000 gpm was found to be more suitable in the present experiments. Krishnamurti *et al.* (1978) have also suggested the same value for the GATE area.

4. Results of experiments in initialization

Since the results of the initialization and forecast experiments are similar for both synoptic situations, only the results for 4 August 1968 will be presented in this paper, but wherever necessary the results of 5 August 1968 will be discussed.

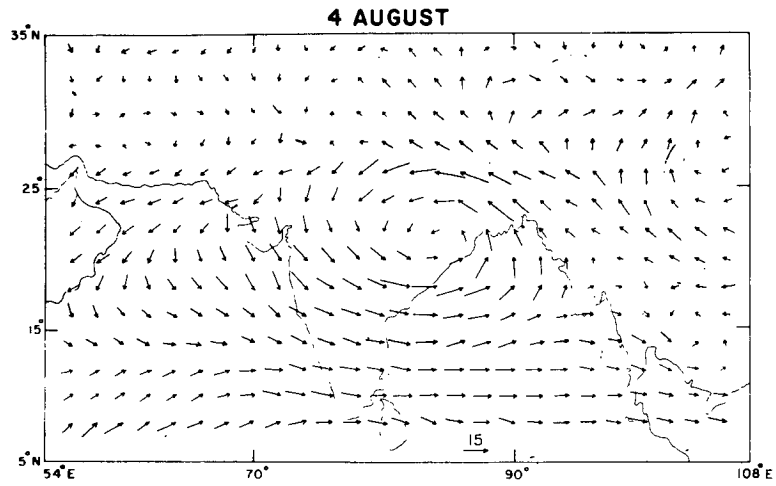

FIG. 1. Observed 700 mb wind vector (m s^{-1}) field at 0000 GMT, 4 August 1968.

a. Dynamic initialization

Fig. 2 presents the dynamically initialized 700 mb wind and geopotential height fields at 0000 GMT 4 August 1968. The figure reveals that all map features of the observed wind are retained in the dynamically initialized wind with more or less same intensity. Thus, the basic desirability of any initialization scheme that the difference between balanced and unadjusted input parameter (wind in this case) should be small is satisfied. Fig. 3 presents the rms difference of two successive iterations of the u and h fields for various iterations. The rms difference for all fields rapidly decreases for the first few iterations and then decreases rather slowly. Toward the end, the percentage decrease is nearly 10% which suggests that convergence of the scheme has been achieved. Similar criteria were utilized by Kanamitsu (1975) and Carr (1977) in their tropical prediction models.

Table 1 gives the numerical value of the conservative quantities of the model, *viz.*, the mean potential vorticity, mean-square potential vorticity, and mean total energy at various stages of the dynamic initialization. In addition, the mean absolute value of divergence for the whole domain and for the region covered by cyclonic flow are also presented in the table. Small fluctuations in the conservative quantities suggest that the numerical model experiment satisfactorily preserves these domain-averaged quantities.

Mean divergence decreases continuously throughout the experiment which is due to geostrophic adjustment between mass and motion fields. While

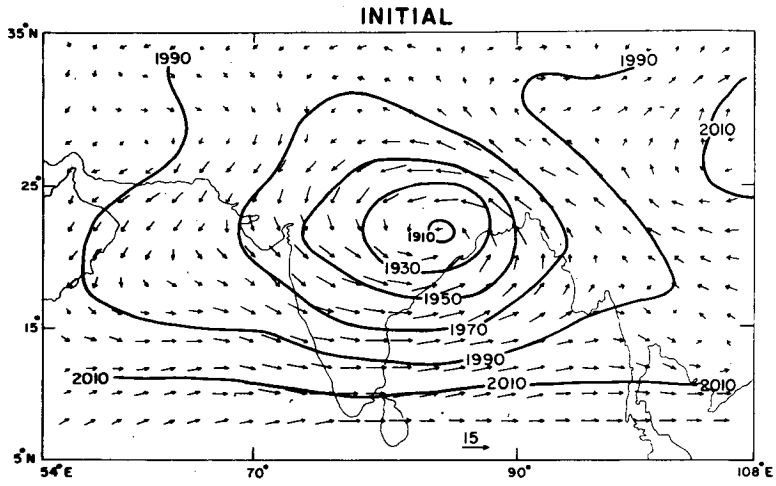

FIG. 2. Initial 700 mb wind vector (m s^{-1}) and geopotential height (gpm) fields at 0000 (GMT), 4 August 1968 for dynamically initialized fields (Scheme V).

comparing the observed wind field with the finally adjusted wind field after the dynamical initialization, it is found that the total wind field did not show much change. It is also observed that the rate of decrease of mean divergence over the entire domain during the initialization was comparable with that over the cyclonic domain. In addition, at the end of the experiment weak divergence (Table 1) is retained over the region.

b. Comparison of initialization schemes

Nondivergent wind and corresponding balanced geopotential height fields are shown in Fig. 4. Geopotential height fields (presented only for Schemes IV and V in Figs. 4 and 2, respectively) derived from Schemes I–V show that the flow patterns remain similar in all the schemes although individual values and the horizontal gradients are slightly different from each other. As far as the wind field is concerned there is a remarkable difference in the intensity of the wind from static (Fig. 4) to dynamic initialization experiments. The latter scheme yields stronger wind fields than the former, which is understandable since the static initialization scheme retains only the nondivergent part of the wind, whereas the dynamic initialization incorporates the total wind (nondivergent and divergent parts).

In order to examine the height fields more critically, height differences between two successive schemes (higher balance approximation minus lower balance approximation) were obtained for the cyclonic region and are presented in Fig. 5. Furthermore, the height gradient around the depression was computed for each scheme and is presented in Table 2. The location and the absolute value of the height at the center of the monsoon depression are also presented in Table 2. It may be seen from Fig. 5 and Table 2 that major adjustment in the initialization experiments takes place from Schemes I to II and from Schemes III to IV. However, from Schemes II to III and IV to V insignificant change in the height value and in the gradient may be noted. Although nonlinear terms lower the absolute value of the height field in the balance equation solution, it improves the gradient considerably.

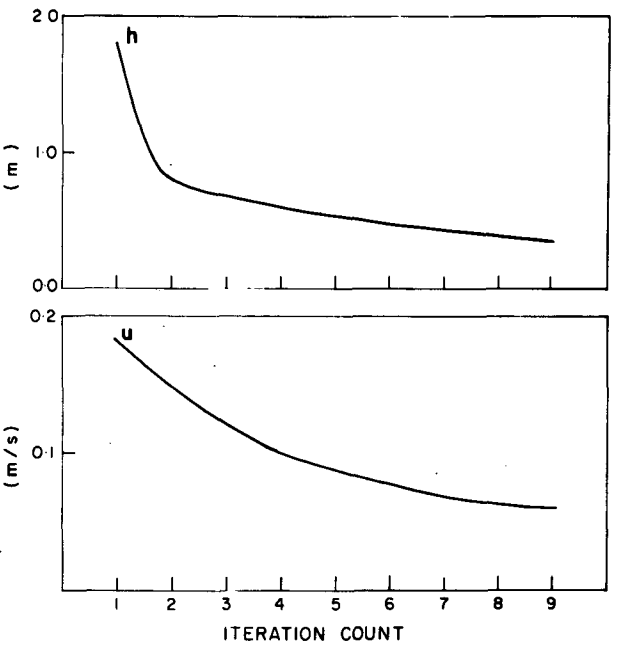

FIG. 3. Root-mean-square difference between two successive iterations using 4 August 1968 input.

For the purpose of more detailed evaluation of initialized fields with observed data, divergence and vorticity of the observed and initialized fields were computed and are presented in Fig. 6. Since

TABLE 1. Variations of mean potential vorticity, mean square potential vorticity, mean total energy, mean absolute divergence for the whole domain and mean absolute divergence for the cyclonic domain (from latitude 16–28°N and longitude 74–94°E) during the dynamic initialization experiments.

Iteration no.	Time step	Mean potential vorticity (10^{-8} m^{-1} s^{-1})		Mean square potential vorticity (10^{-16} m^{-2} s^{-2})		Mean total energy (10^{-7} m^{3} s^{-2})		Mean total divergence (10^{-6} s^{-1})			
								Whole domain		Cyclonic domain	
		4 Aug	5 Aug	4 Aug	5 Aug	4 Aug	5 Aug	4 Aug	5 Aug	4 Aug	5 Aug
1	20	2.675	2.693	8.471	8.456	1.945	1.956	5.479	5.506	3.274	6.091
2	40	2.675	2.693	8.470	8.455	1.945	1.956	4.478	4.577	2.468	5.028
3	60	2.675	2.693	8.469	8.454	1.945	1.956	3.800	3.922	1.946	4.316
4	80	2.675	2.692	8.469	8.453	1.945	1.956	3.316	3.449	1.597	3.842
5	100	2.675	2.692	8.468	8.452	1.945	1.956	2.959	3.106	1.402	3.486
6	120	2.675	2.692	8.467	8.451	1.945	1.956	2.687	2.851	1.271	3.220
7	140	2.675	2.692	8.467	8.451	1.945	1.956	2.471	2.657	1.174	3.009
8	160	2.675	2.692	8.466	8.450	1.945	1.956	2.300	2.501	1.114	2.828
9	180	2.675	2.692	8.466	8.449	1.945	1.956	2.161	2.371	1.084	2.676

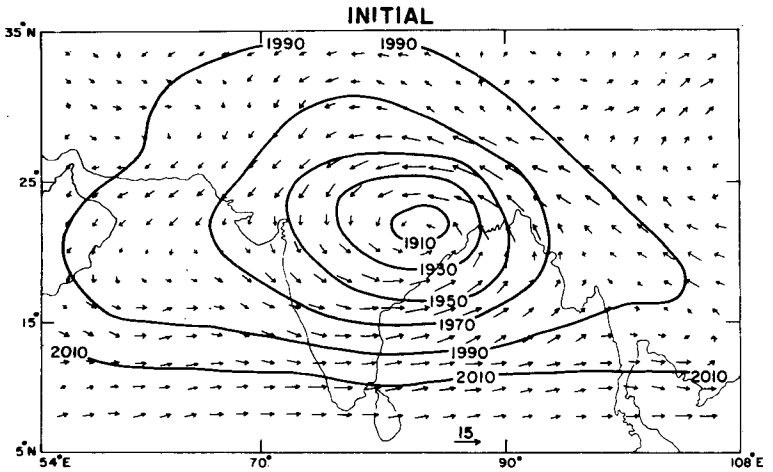

FIG. 4. Initial 700 mb wind vector (m s^{-1}) and geopotential height (gpm) fields at 0000 GMT, 4 August 1968 for statically initialized fields (Scheme IV).

the divergence of the statically initialized (nondivergent) wind is zero, only the divergence fields from the observed and dynamically initialized fields are presented. Similarly as the observed winds are used for the computation of the relative vorticity which in turn is used to obtain the streamfunction, the relative vorticity field of the nondivergent wind is also not presented.

The relative vorticity field of the observed wind (Fig. 6a) shows a region of positive vorticity extending southwest from the Arabian sea toward the north Bay of Bengal and then to southeast Asia across central India. The dominant maximum in this field lies near 22°N, 85°E very close to the center of the monsoon depression. The vorticity of the dynamically initialized wind field (Fig. 6b) is in

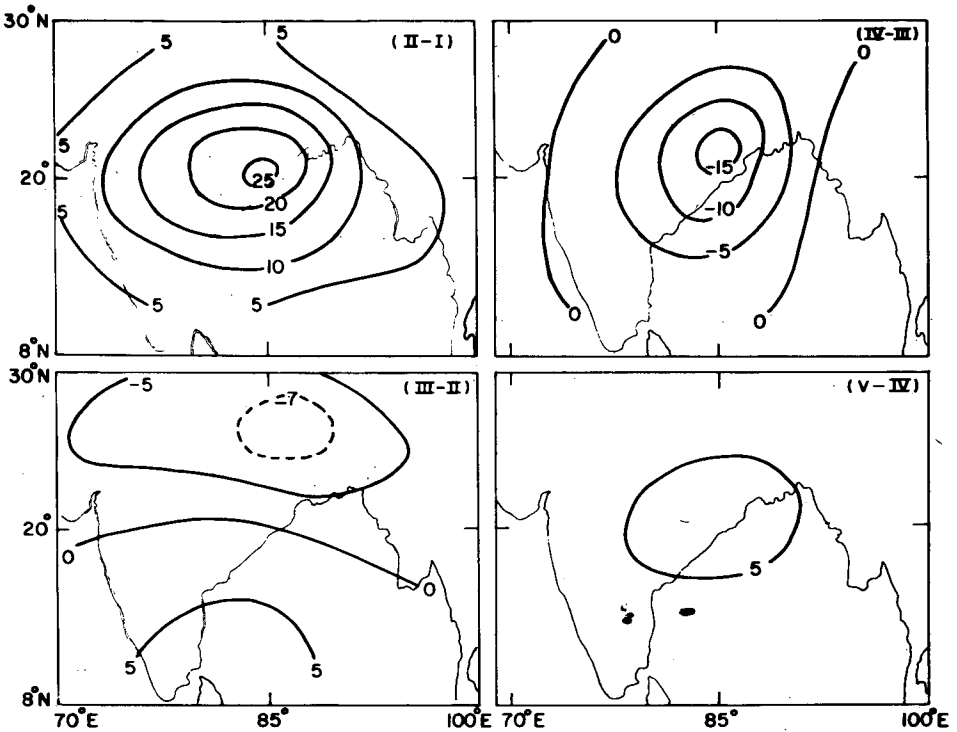

FIG. 5. Difference in geopotential height (gpm) field in two successive initialization schemes (using 4 August 1968 input).

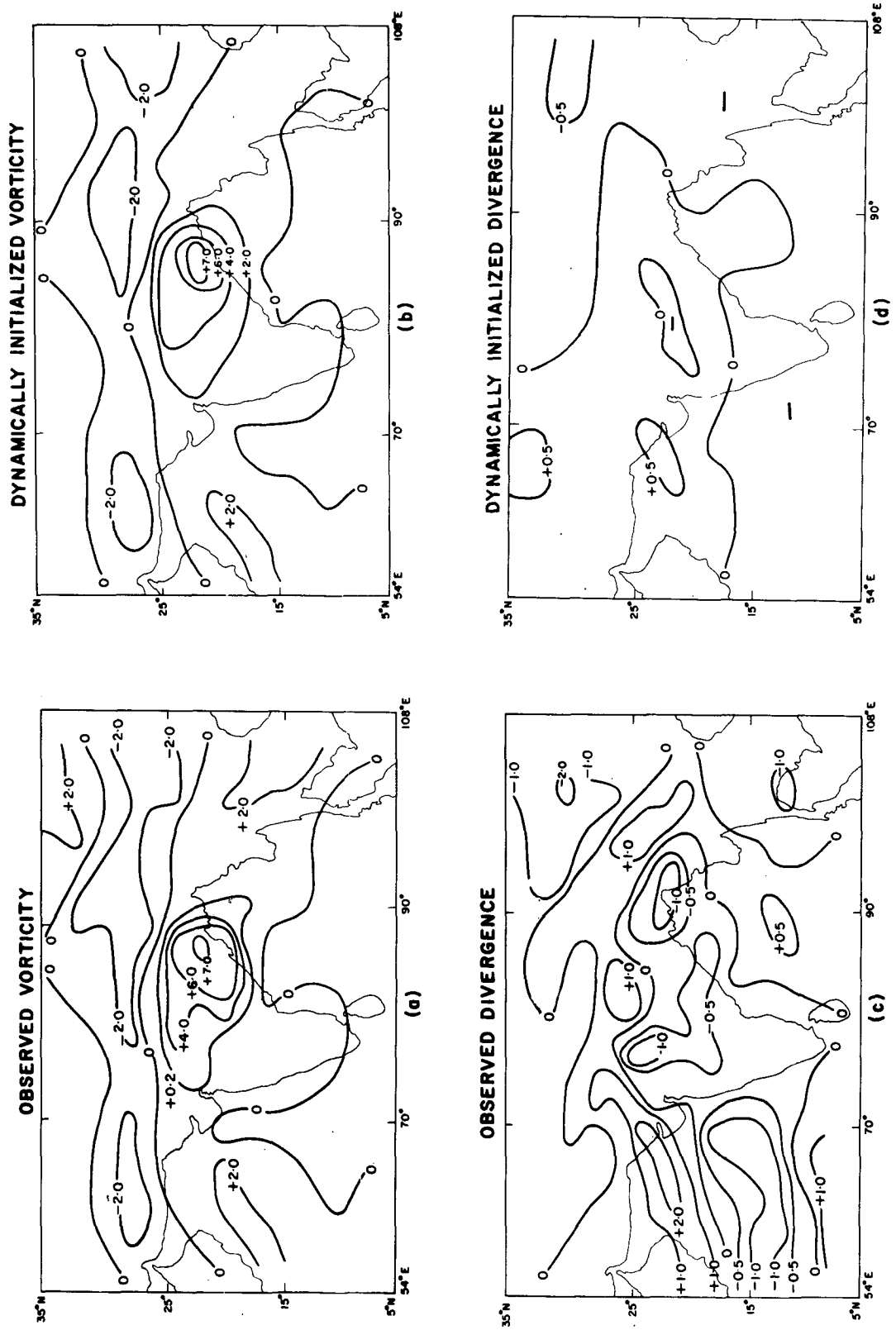

FIG. 6. Divergence (10^{-5} s^{-1}) and relative vorticity (10^{-5} s^{-1}) of observed and dynamically initialized wind fields using 4 August 1968 input.

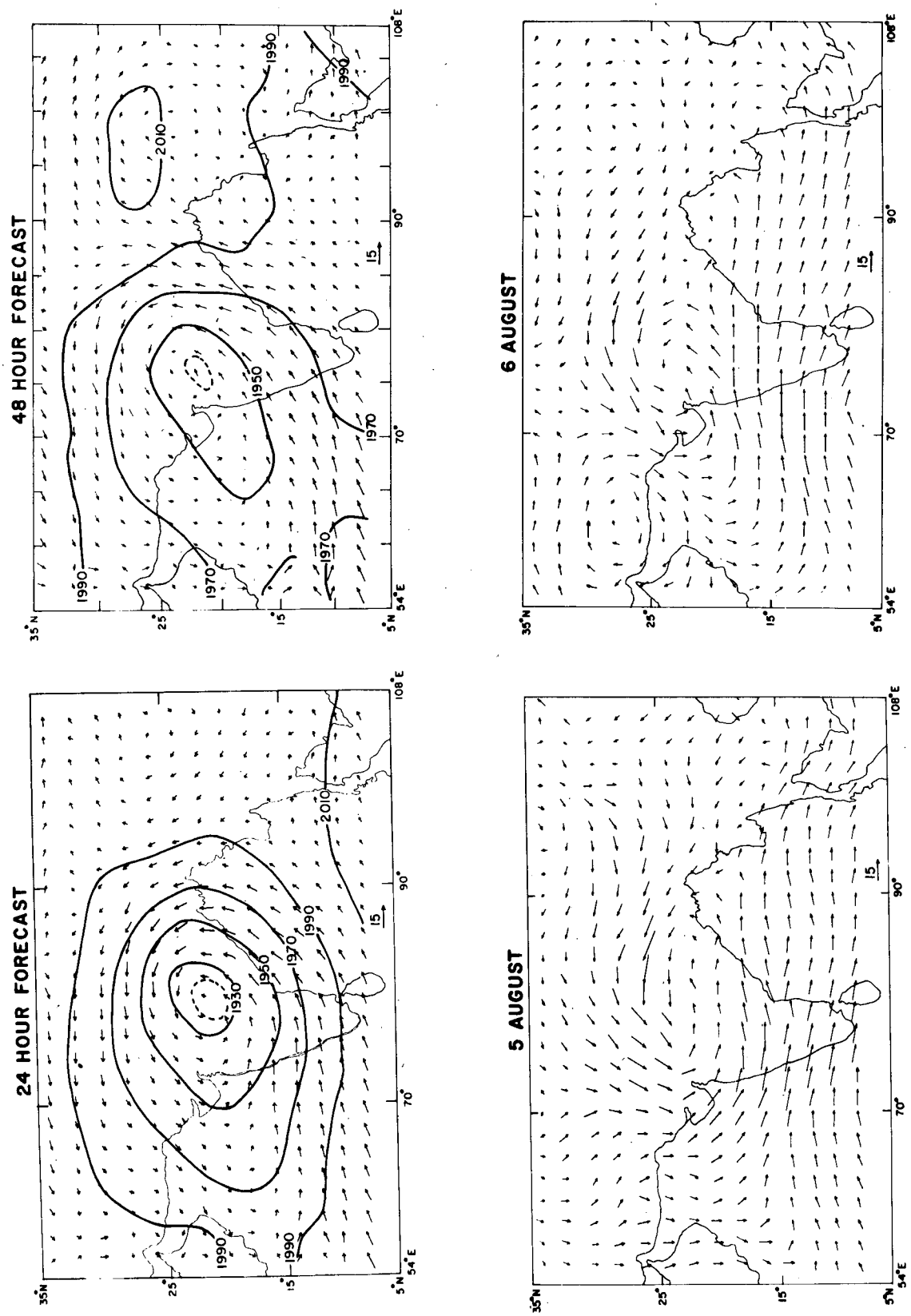

FIG. 7. The 24 and 48 h forecasts of wind vectors (m s^{-1}) and geopotential height (gpm) fields and corresponding verification wind vector fields (the initial map is given in Fig. 4).

TABLE 2. Geopotential height at the center of depression, location and height gradient ($\partial h/\partial x, \partial h/\partial y$) obtained in various schemes of initialization.

Scheme	I	II	III	IV	V
	(Input: 700 mb 0000 GMT, 4 August 1968)				
Height values at the center (gpm)	1902	1926	1923	1906	1909
Location of the center	22°N, 83°E	22°N, 83°E	22°N, 83°E	22°N, 83°E	22°N, 83.5°E
Height gradient (10^{-5})	7.9 (N-S) 5.2 (E-W)	5.7 (N-S) 3.5 (E-W)	5.8 (N-S) 3.3 (E-W)	7.5 (N-S) 5.1 (E-W)	7.6 (N-S) 5.2 (E-W)
	(Input: 700 mb 0000 GMT, 5 August 1968)				
Height values at the center (gpm)	1905	1927	1923	1910	1914
Location of the center	23°N, 79°E	23°N, 79°E	23°N, 79°E	23°N, 79°E	23°N, 79°E
Height gradient (10^{-5})	6.4 (N-S) 4.2 (E-W)	5.0 (N-S) 3.2 (E-W)	5.5 (N-S) 3.3 (E-W)	7.4 (N-S) 4.8 (E-W)	6.9 (N-S) 4.7 (E-W)

excellent agreement with the observed vorticity both in the pattern as well as in corresponding magnitudes. However, the former pattern is smoother than the latter as expected.

The observed divergence pattern as depicted in Fig. 6c shows a zone of convergence extending from the Arabian sea southwest toward the north Bay of Bengal which is associated with the monsoon trough. A region of convergence also lies near the northeast corner of the domain over China in association with a cyclonic circulation existing over there. It may be noted that over the domain as a whole as well as over the region of the cyclonic domain, divergence is rather weak. This is so because the 700 mb level is close to the level of nondivergence for the monsoon flow. The divergence field of the dynamically initialized wind (Fig. 6d) is considerably reduced as expected and the reduction is about half the magnitude compared to the observed divergence. This indicates that the dynamical initialization procedure has retained only a very small part of the divergence of the observed winds. The minor difference between Schemes IV and V, with respect to the absolute value and gradient of geopotential height, divergence and vorticity indicates that for a barotropic model balance equation static initialization is quite effective and dynamic initialization brings very little improvement in the initial field. This aspect will be discussed further in Sections 5 and 6. However, it may be noted that in this experiment our chief synoptic feature lies sufficiently away from the equator. Therefore, to test the validity of the nonlinear balance *vis-a-vis* dynamic initialization, a well-documented case study of a low-latitude synoptic-scale feature would be more desirable.

5. Forecast results

Fig. 7 presents 24 and 48 h forecast wind and geopotential height fields and corresponding verification wind fields with input from Scheme IV and Fig. 8 gives the 24 and 48 h forecast wind fields corresponding to Scheme V. Initial 24 and 48 h forecast positions of the center of the monsoon depression for both synoptic situations as obtained from the two schemes are presented in Table 3.

It may be noted from Figs. 7 and 8 that, in general, the forecast fields from both schemes are quite satisfactory up to 48 h and beyond that (not presented) they are found to deteriorate quickly. However, it is apparent that the geometry of the circulation features is better preserved in the case of the forecasts based on the input from the dynamic initialization scheme. This is particularly so for the 48 h forecast as can be readily judged from the intensity and the extension of the ridge line along 92°E to the east of the monsoon depression. Better representation of intensity and geometry of the circulation features, a desirable feature in any dynamical forecast, has been found to be a definite advantage of the dynamic initialization scheme in this series of experiments.

Table 3 shows that the movement of the monsoon depression up to 48 h is predicted with a fair degree of accuracy by both the schemes. However, in case of the second synoptic situations on 5 August 1968, both schemes did not yield as good a result as in the case of the situation on 4 August 1968.

6. Concluding remarks

The result that emerges from the present study suggests that the dynamical initialization scheme is either slightly superior or comparable to that of static initialization (application of the nonlinear balance equation). Although the application of static initialization for balancing mass and wind fields for divergent barotropic models is quite adequate, a better representation of the geometry of the circulation features at 48 h, brought out by dynamic

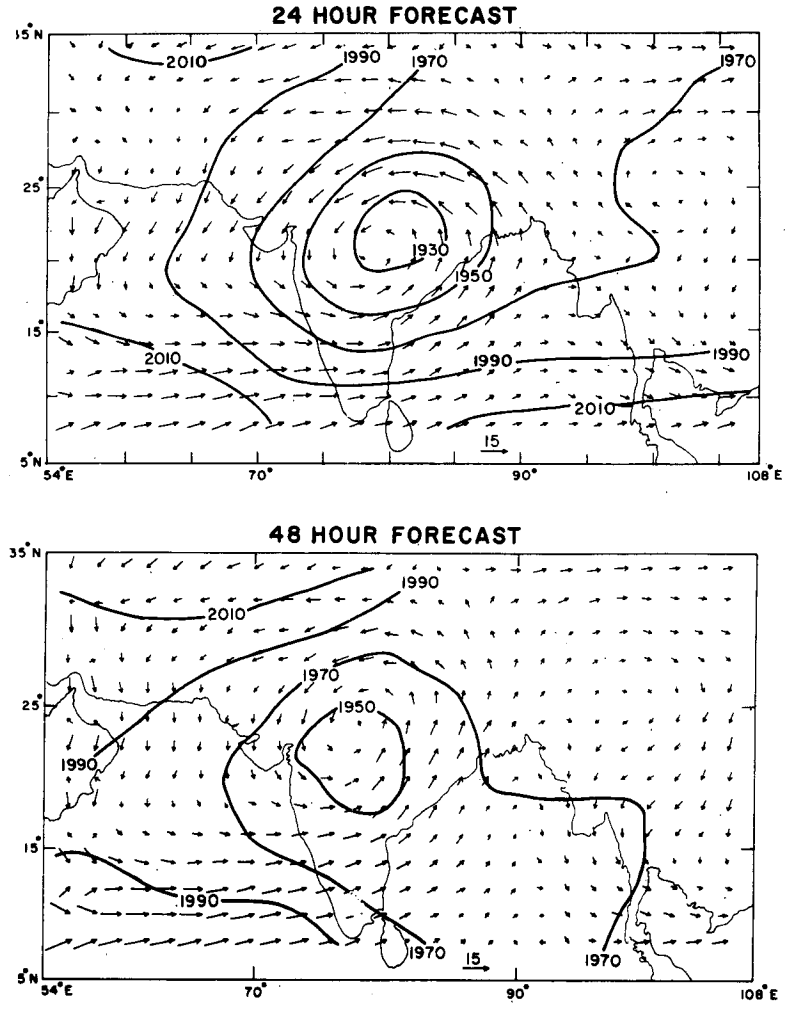

FIG. 8. The 24 and 48 h forecasts of wind vectors (m s^{-1}) and geopotential (gpm) fields [the initial map is given in Fig. 2 and verification wind vector (m s^{-1}) fields are shown in Fig. 7].

initialization, might be useful for longer time integration, say, up to 96 h. The longer range of useful forecasts that would be expected from the application of the dynamic initialization scheme, was actually not found in this experiment. Perhaps, the domain of integration is too small to yield a good forecast beyond 48 h. Thus, it is desirable to examine whether the application of the dynamic initialization

TABLE 3. Forecast and observed position of the center of the monsoon depression.

Time	Observed position	Balance initialization		Dynamic initialization	
		Position	Vector error (km)	Position	Vector error (km)
		(Input: 700 mb 0000 GMT, 4 August 1968)			
Initial time	21.5°N, 83°E	21.5°N, 83°E	0	21.5°N, 83°E	0
24 h	23°N, 79°E	22°N, 79°E	110	22.0°N, 79°E	110
48 h	23°N, 76°E	24°N, 76°E	110	24°N, 76°E	110
		(Input: 700 mb 0000 GMT, 5 August 1968)			
Initial time	23°N, 79°E	23°N, 79°E	0	23°N, 79°E	0
24 h	23°N, 76°E	22°N, 78°E	220	22°N, 76°E	110
48 h	24°N, 72°E	24°N, 76°E	440	24°N, 74°E	220

scheme improves the range of useful forecast with the following refinements in the model:

- Extension of domain in east-west and north-south directions.
- Inclusion of the effects of terrain in the model.
- Reduction of grid size from 2 to 1° latitude-longitude.

Experiments on the above aspects with a better set of data from ISMEX-73 and the Monsoon-77 Experiment are in progress and the results will be reported later.

The results of the present study demonstrate the following:

1) Feasibility of dynamic initialization for a limited-area primitive equation barotropic model has been proposed.

2) Geopotential height fields derived by Schemes I–V give similar flow features in all schemes with different height gradient.

3) Forecast by the dynamic initialization scheme is either slightly superior or comparable to that of the static initialization scheme. The range of useful forecasts could not be improved with application of the new scheme.

4) It appears that the nonlinear balance equation solution is quite adequate to bring about balance between wind and mass fields for a one-level primitive equation model.

Acknowledgments. The authors would like to thank the Director, Indian Institute of Tropical Meteorology, for his interest in this study and to Shri A. Bandopadhyay for assisting in the preparation of diagrams. They also wish to thank Shri A. Girijavallabhan for typing the manuscript and Shri V. V. Deodhar who drafted the diagrams.

REFERENCES

Baer, F., 1977: Adjustment of initial conditions required to suppress gravity oscillations in nonlinear flows. *Contrib. Atmos. Phys.*, **50**, 350–366.

——, and J. Tribbia, 1977: On complete filtering of gravity modes through nonlinear mode initialization. *Mon. Wea. Rev.*, **105**, 1536–1539.

Carr, F. H., 1977: Numerical simulation of a mid-tropospheric cyclone. Rep. 77-1, Dept. of Meteorology, Florida State University, 106 pp.

Charney, J. G., 1955: The use of the primitive equations of motion in numerical prediction. *Tellus*, **7**, 22–26.

Hinkelmann, K., 1959: Ein numerisches experiment mit den primitiven Gleichungen. *C. G. Rossby Memorial Volume*, Oxford University Press, 486–500.

Kanamitsu, M., 1975: On numerical prediction over global tropical belt. Rep. 75-1, Dept. of Meteorology, Florida State University, 97 pp.

Krishnamurti, T. N., H. L. Pan, C. B. Change, J. Ploshay, D. Walker and A. W. Oodally, 1978: Numerical weather prediction for GATE. Rep. 77-7, Dept. of Meteorology, Florida State University, 15 pp.

Kiangi, P. M. R., 1977: Some aspects of initialization using real tropical wind data. *Arch. Meteor. Geophys. Bioklim.*, **A26**, 349–360.

Machenhauer, B., 1977: On the dynamics of gravity oscillations in a shallow water model with application to normal mode initialization. *Contrib. Atmos. Phys.*, **50**, 253–271.

Mesinger, F., 1972: Computation of wind by forced adjustment of the height field. *J. Appl. Meteor.*, **11**, 60–71.

Miyakoda, K., and R. W. Moyer, 1968: A method of initialization for dynamic weather forecasting. *Tellus*, **20**, 115–128.

Nitta, T., and J. B. Hovermale, 1969: A technique of objective analysis and initialization for primitive forecast equations. *Mon. Wea. Rev.*, **79**, 79–84.

Phillips, N. A., 1960: On the problem of initial data for the primitive equations. *Tellus*, **12**, 121–126.

Ramanathan, Y., and K. R. Saha, 1972: Applications of a primitive equation barotropic model to predict movement of western disturbances. *J. Appl. Meteor.*, **11**, 268–272.

Shuman, F. G., 1962: Numerical experiments with the primitive equations. *Proc. Int. Symp. Numerical Weather Prediction*, Toyko, Meteor. Soc. Japan, 85–107.

Singh, S. S., 1977: Some aspects of prognostic and diagnostic studies of Indian summer monsoon. Ph.D. Thesis, Banaras Hindu University, Varanasi, India, 32–74.

——, and K. R. Saha, 1976: Numerical experiments with primitive equation barotropic model to predict the movement of monsoon depressions and tropical cyclones. *J. Appl. Meteor.*, **15**, 805–810.

Williamson, D. L., and R. E. Dickinson, 1976: Free oscillations of the NCAR global circulation model. *Mon. Wea. Rev.*, **104**, 1370–1391.

Winninghoff, F. J., 1973: Note on a simple restorative procedure for initialization of a global forecast model. *Mon. Wea. Rev.*, **79**, 79–86.